Robot Calibration Using Relative Measurements

David Chao-Chia Lu* M. John D. Hayes†
Carleton University Carleton University
Ottawa, Canada Ottawa, Canada

Abstract— *Kinematic calibration is necessary to enhance the accuracy of robotic manipulators. It is typically desired to perform this task in both a cost-effective and time-efficient manner. Many techniques exist in the literature that achieve both goals using absolute measurements. In this paper, a modified model-based kinematic calibration method using optically obtained relative measurements is developed and implemented on a 7 DOF WAM Arm. Results indicate that it is capable of achieving approximately the same level of accuracy as some absolute measurement methods. Moreover, the calibration method presented in this paper leads to quantifiable improvement in both the positioning and orienting accuracy. The implication is that the relative measurement concept is a valid tool for model-based kinematic calibration of serial manipulators, and the results presented herein are it's first empirical validation.*

Keywords: robotics, kinematics, calibration, serial manipulators, hand-eye calibration, relative measurements, parameters estimation

I. Introduction

Robot manipulator calibration has been an active research topic for many years. It is highly essential for robot manufacturing systems, because manipulators generally have vastly superior repeatability compared to their accuracy, which can render them unfeasible for some applications. Repeatability is the ability of the robot to return to the same taught end-effector position and orientation (pose) where the joint angles are taught to the robot and stored in the controller. Conversely, accuracy is a measure of how well the robot controller can place the end-effector in a prescribed pose where the required robot joint angles must be computed using the nominal kinematic model embedded in the controller. The goal of robot kinematic calibration is to identify and compensate errors in the nominal kinematic model so that its accuracy can be improved. The bound on accuracy improvement is the repeatability of the robot, which is typically quantified by the manufacturer using the standard deviation of positioning error upon returning to taught positions over the breadth of its reachable workspace using a statistically viable set of taught positions [1].

The manipulator pose accuracy can be affected by geometric and non-geometric errors [2]. Geometric errors are artifacts of the joint offsets and the errors in the nominal kinematic parameters. Non-geometric errors, on the other hand, are typically due to friction, inertia, applied load, flexibility, and temperature induced dimensional deformation. Experimental results reported in [2] conclude that about 95% of manipulator inaccuracies are due to the geometric errors. This leads to the motivation for this paper to be focused on the development of a method using relative measurements to identify the errors in the kinematic geometry of serial robot manipulators to enhance position and orientation accuracy.

*chaochialu@cmail.carleton.ca
†jhayes@mae.carleton.ca

II. Background

Improving the pose accuracy of a robot manipulator using kinematic calibration has been an active research topic since the introduction of industrial robots in the early 1960s [1]. Researchers have addressed issues regarding kinematic calibration methods, measurement methods [3], [4], [5], [6], [7], [8], kinematic models [9], [10], [11], and parameter identification methods [12], [13]. This paper focuses mainly on the kinematic calibration methods.

A. Kinematic Calibration

A wide variety of different kinematic calibration methods have been developed over the past few decades, several relevant approaches are described next.

A.1 Relative Measurement

The concept devised by Hayes and O'Leary [14] and reported in [15] was the first work found on kinematic calibration using relative position measurements. In this work, the calibration method was applied to a KUKA KR-15/2 6R serial robot. The pose measurement was achieved by having the robot draw lines in its base frame's $\mathbf{x}$ and $\mathbf{y}$ directions and rigidly mounting two precision-ruled straight edges parallel to these directions, as well as a flat standard mounted on its Bernoulli points so that it does not deform under its own weight. A CCD camera and two MEL laser displacement sensors were attached to a fixture mounted to the tool flange. The relative position measurements of the $\mathbf{x}$ and $\mathbf{y}$ components can be extracted from the CCD camera images, while the relative change in the $\mathbf{z}$ component was measured by two MEL laser displacement sensors. However, at this point of the work, only simulated measurement runs converged to solutions, while the empirical results were not successful: the sets of three relative

displacement errors applied to the identification equations wold not converge to realistic values.

Simpson [16] continued the work proposed in [15], which instead used only a CCD camera on the end-effector of a Thermo CRS A465, and only relative displacement measurements in the robots base frame $\mathbf{x}$ and $\mathbf{y}$ directions. The robot was commanded to move the end-effector along the length of the precision-ruled straight edge in increments 1 cm. The straight edge was placed carefully such that the first increment was aligned with the centre of the image taken by the CCD camera. For every 1 cm increment that the end-effector moved, the corresponding observed misalignment of ruling lines on the straight edge between two subsequent images represents the relative position error scaled by the straight edge itself along its length. In this work, calibration was attempted using both the simulated data and the experimental data. Like [14], the simulations were successful, whereas the experimental results yielded solutions that diverged away from the nominal parameters, presumably because of poor conditioning in the identification equations.

Ha [17] on the other hand, approached relative position measurement a little differently. Instead of relying on the correct placement of measurement tools, Ha developed a suitable kinematic error model for recognizing the relative position errors. The experiment consists of a six DOF manipulator (MOTOMAN UP 20), a laser displacement sensor (accuracy of ± 0.01 mm) and a machined grid plate (accuracy of ± 0.1 mm). In this work, it was concluded that the relative measurement concept can be performed without the knowledge of the position of the robot base, but the orientation of the robot base is still required knowledge.

A.2 Inverse Calibration Method

Inverse calibration was developed to determine the errors observed in the end-effector poses, and use them to estimate the required joint angles to compensate for the errors [18], [19], [20], [21]. With this method, no effort is invested in correcting the manipulator model, rather approximation functions for the end-effector errors are determined. Therefore, this method can also be referred to as a non-parametric accuracy compensation [22]. The approximation functions have no direct physical meaning because they consist of components of both the geometric and non-geometric errors.

For a six DOF manipulator, the approximation functions are defined using a multivariate polynomial with six variables, which is quite complex. Shamma and Whitney [18] developed a method for six DOF wrist-partitioned manipulators by considering two computationally independent parts: the calibration of the shoulder and the wrist. This simplifies the approximation functions of the multivariate polynomial into two polynomials factors. Doria *et al.* [19] defined multiple second order spline functions, piecewise polynomials, to approximate the multivariate polynomials. Zhong *et al.* [20], on the other hand, applied a feed-forward artificial neural network to estimate the approximation functions.

Dolinsky [21] examined all the inverse calibration methods and observed that numerical estimation techniques can be compromised by numerical instability. Dolinsky then proposed a method for determining the approximation functions with genetic programming, which uses stochastic methods to symbolically generate the functions.

A.3 Circle Point Analysis

This method estimates the line equations of robot revolute joint axes for an arbitrary robot configuration by estimating the circle drawn out by each robot joint [22], [23]. Because a least-squares technique is used to estimate each circle, more than three points are required. However, since the trajectory of the end-effector is not, in general, a circle if multiple joints are in motion simultaneously, the robot must be moved one joint at a time.

The true kinematic model parameters can be extracted from the line equations defining the joint axes. Two strategies have been developed to extract the kinematic parameters from the identified joint axes. The first, Stone [23], consists of deriving an analytical formula for the kinematic parameters in terms of the link homogeneous transformation matrices. The second, Sklar [24], [25], consists of computing common normal lengths, offset distances, and twist angles directly from the identified line equations using standard vector algebra relationships and the existing geometrical constraints.

Kim *et al.* [26] reviewed the work from Stone and Sklar on circle point analysis, and they conducted an experiment using a HYUNDAI robot AE 7601 and KIMI-tester (a type of CMM). The experiment showed that the circle point analysis technique is capable of improving the absolute positioning accuracy of the robot by an order of magnitude, from standard deviations of 10 mm to 1 mm over the entire manipulator workspace. However, orienting accuracy is not included.

III. New Relative Kinematic Calibration Approach

Let the actual kinematic geometry of the robot be represented by Model A and let Model B be the nominal kinematic geometry parameters embedded in the robot controller. The pose arrays whose elements are the linearly independent coordinates of position and orientation of the end-effectors for the actual and nominal robots are $\boldsymbol{x}_A$ and $\boldsymbol{x}_B$, respectively. The aim of the kinematic calibration is to minimize the errors between $\boldsymbol{x}_A$ and $\boldsymbol{x}_B$.

A reasonable approach is to approximate $\boldsymbol{x}_A$ using the Taylor series expansion about the pose computed in the controller using some form of nominal Denavit-Hartenberg (DH) kinematic parameters [27], $\boldsymbol{\zeta}_n$. That pose, $\boldsymbol{x}_n$, is ap-

proximated as

$$\boldsymbol{x}_A \approx \boldsymbol{x}_B = \boldsymbol{x}_n + \Delta\boldsymbol{x} = \boldsymbol{f}(\boldsymbol{\zeta}_n) + \frac{\partial \boldsymbol{f}}{\partial \boldsymbol{\zeta}}\Delta\boldsymbol{\zeta} + HOT, \quad (1)$$

where $\Delta\boldsymbol{\zeta}$ are the estimated errors in the nominal kinematic parameters, and HOT represent all higher order terms. The complete 6 DOF pose in Eq. (1) consists of three position component elements contained in the array ($\Delta\boldsymbol{p}$) and three orientation component elements contained in ($\Delta\boldsymbol{\Phi}$). Because all component elements are linearly independent allows one to approach the problem by using partial pose measurement, for example many methods in the literature use only position measurements. Since the errors in the kinematic model are expected to be quite small compared to the nominal parameters, the HOT may be ignored because they are negligibly small, possibly on the same order of magnitude of the numerical resolution of the computers used.

A. *Two Fundamentally Different Measurement Approaches*

Broadly speaking, it may be said that the goal of kinematic calibration is to determine the $\Delta\boldsymbol{\zeta}$ that minimizes $\Delta\boldsymbol{x}$. Because the functional relationship between $\boldsymbol{x}_B$ and $\boldsymbol{\zeta}$ is nonlinear, many measurements of $\boldsymbol{x}_A$ are needed to converge to a useful solution. In this section, two approaches to acquiring measurements used for identifying the errors in the kinematic model are presented. First, the conventional absolute measurement approach is reviewed, then the proposed relative measurement approach is presented.

A.1 *Conventional Absolute Measurement Approach*

Consider a manipulator that is commanded to move through a series of configurations. At configuration i, the poses, $\boldsymbol{x}_{A,i}$ and $\boldsymbol{x}_{B,i}$, are produced. That is, the i^{th} pose of the actual robot represented by Model A and expressed as $\boldsymbol{x}_{A,i}$ is somehow measured relative to a known stationary coordinate system, here called the metrology frame Σ_m. Whereas the corresponding i^{th} pose of the DH based Model B, $\boldsymbol{x}_{B,i}$ is computed by the controller using forward kinematics, and is expressed with respect to the manipulator base frame Σ_b.

In order to determine the pose errors between the two, both poses must be with respect to the same reference frame. A fixed world frame Σ_w is introduced as the common reference for the two poses, then the pose errors are

$${}^w\boldsymbol{e}_i = {}^w\boldsymbol{x}_{A,i} - {}^w\boldsymbol{x}_{B,i} = \begin{bmatrix}\Delta^w\boldsymbol{p}_i & \Delta^w\boldsymbol{\Phi}_i\end{bmatrix}^T, \quad (2)$$

where ${}^w\boldsymbol{e}_i$ is the *absolute error* of the i^{th} pose described in Σ_w, which can be an array containing both position and orientation errors, or any subset thereof. The kinematic calibration performed using the absolute error is referred to as the *absolute measurement concept* or *AMC*. Fig. 1 uses two chessboards as the conceptual representation of the measurement system to illustrate the absolute error.

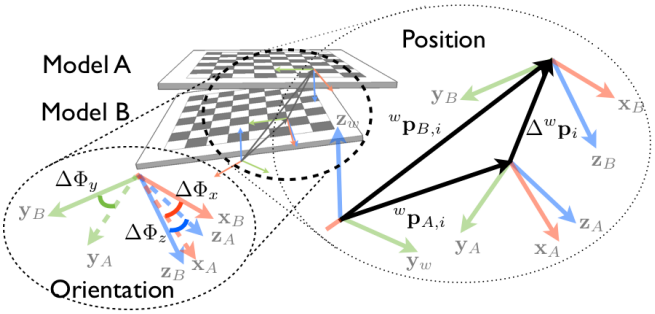

Fig. 1. Exaggerated representation of absolute pose errors.

In most of the approaches described in the literature, the measurement system frame Σ_m is used as the world frame Σ_w. This means that additional measurements are required to establish the relationship between Σ_b and Σ_m.

A.2 *Proposed Relative Measurement Approach*

The objective set out for the work presented herein is to develop a simple, low cost, kinematic calibration method that does not rely on absolute measurements. The approach proposed here builds on the work in [16], [17], which used only $\mathbf{x}$ and $\mathbf{y}$ components of relative position measurements. In this work, all six linearly independent position and orientation components in the relative pose measurements are used to enhance the precision of the identified errors.

Fig. 2 Illustrates the setup for implementing this approach to kinematically calibrate a 7 DOF WAM Arm with a manufacturer stated repeatability of ± 0.2 mm. As shown in the figure, a target object, or calibration board, was placed on the end-effector of the robot, and a camera placed outside of the robot's workspace such that the target object can always be viewed. Because it is simpler to manufacture a precise 2D registration object than a 3D object, a chessboard patterned object used for camera calibration [28] was chosen, and used to establish the pose of the target object relative to the camera. This pose information was then used to estimate the end-effector pose of the Wam Arm.

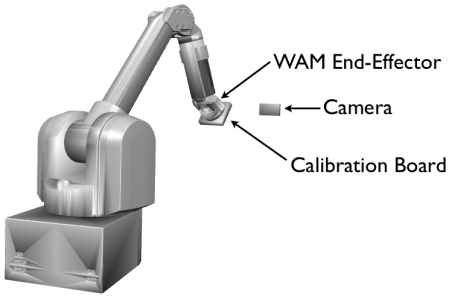

Fig. 2. The relative measurement setup for the 7 DOF WAM Arm.

Now that an experimental setup can be visualized, con-

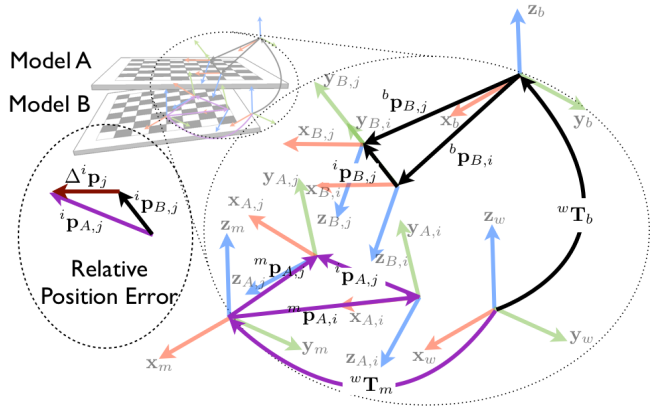

Fig. 3. Exaggerated relative position errors.

sider the manipulator is commanded to move through the same series of configurations as those that would be used in the conventional approach, where the configuration j is next from i, producing two new poses of Models A and B, $\boldsymbol{x}_{A,j}$ and $\boldsymbol{x}_{B,j}$. Fig. 3 uses two chessboards illustrating relative position measurements between i and j.

The end-effector poses, $\boldsymbol{x}_A$ and $\boldsymbol{x}_B$, are expressed relative to a common reference frame, Σ_w. The end-effector position j relative to i can be obtained from the vector differences,

$$^{i}\boldsymbol{p}_{A,j} = {}^{w}\boldsymbol{p}_{A,j} - {}^{w}\boldsymbol{p}_{A,i}, \tag{3a}$$

$$^{i}\boldsymbol{p}_{B,j} = {}^{w}\boldsymbol{p}_{B,j} - {}^{w}\boldsymbol{p}_{B,i}. \tag{3b}$$

The relative position errors are the errors embedded in the two relative positions,

$$\Delta^{i}\boldsymbol{p}_{j} = {}^{i}\boldsymbol{p}_{A,j} - {}^{i}\boldsymbol{p}_{B,j}. \tag{4}$$

The relative orientation errors can be derived similarly to the relative position errors [29]. The relative orientation errors are embedded in the two relative orientations,

$$\Delta^{i}\boldsymbol{\Phi}_{j} = {}^{i}\boldsymbol{\Phi}_{A,j} - {}^{i}\boldsymbol{\Phi}_{B,j}. \tag{5}$$

Similar to the absolute error, both pose errors for robots A and B must also be expressed in the same reference frame. Because both Eqs. (4) and (5) are expressed relative to i, then the errors are

$$^{i}\boldsymbol{e}_{j} = {}^{i}\boldsymbol{x}_{A,j} - {}^{i}\boldsymbol{x}_{B,j} = \begin{bmatrix}\Delta^{i}\boldsymbol{p}_{j} & \Delta^{i}\boldsymbol{\Phi}_{j}\end{bmatrix}^{T}, \tag{6}$$

where $^{i}\boldsymbol{e}_{j}$ is the *relative error* of Pose j relative to Pose i. The kinematic calibration using the relative error is termed the *relative measurement concept* or *RMC* [15], [16], [17], [29].

B. Kinematic Calibration Algorithm

Kinematic calibration algorithms are typically designed for estimating the errors in the kinematic parameters, $\Delta\boldsymbol{\zeta}_B$, such that the differences between $\boldsymbol{x}_A$ and $\boldsymbol{x}_B$ are minimized, ideally to the limit of the robot's repeatability. The most common techniques used to approach this problem are typically some form of nonlinear optimization, such as a nonlinear least-squares methods, genetic algorithm, or singular value decomposition (SVD). Every computation involving the identification of kinematic parameters in this paper are performed using only SVD, which is also a form of least-squares estimation [30].

Given the approximated model as described in Eq. (1), the deviation $\Delta\boldsymbol{x}$ can be linearized by ignoring the higher order terms and collecting all of the partial derivatives into the Jacobian matrix $\mathbf{J}$, giving

$$\Delta\boldsymbol{x} = \mathbf{J}\Delta\boldsymbol{\zeta}. \tag{7}$$

As mentioned previously, a large number of $\boldsymbol{x}_A$ must be measured in order to converge to a useful solution, causing the linearized system above to be overdetermined. The solution of $\Delta\boldsymbol{\zeta}$ can then usually be obtained by applying the Moore-Penrose pseudoinverse of $\mathbf{J}$ [30],

$$\Delta\boldsymbol{\zeta} = \mathbf{J}^{+}\Delta\boldsymbol{x}. \tag{8}$$

If the rows and columns of $\mathbf{J}$ are linearly independent, then $\mathbf{J}^{\mathbf{T}}\mathbf{J}$ is invertible. In this case, Eq. (8) becomes

$$\Delta\boldsymbol{\zeta} = (\mathbf{J}^{\mathbf{T}}\mathbf{J})^{-1}\mathbf{J}^{\mathbf{T}}\Delta\boldsymbol{x}. \tag{9}$$

However, in many practical overdetermined cases, some columns of $\mathbf{J}$ can be linear dependent, or nearly, resulting in $\mathbf{J}^{\mathbf{T}}\mathbf{J}$ being ill-conditioned or singular where the condition number of the Jacobian can approach infinity, i.e., $\kappa(\mathbf{J}) \to \infty$. However, every matrix can be inverted with SVD regardless of condition number [30]. SVD enables a technique for always being able to solve for $\Delta\boldsymbol{\zeta}$ exactly, or estimate it with the minimum least-squares error. The matrix $\mathbf{J}$ can be decomposed into three matrix factors,

$$\mathbf{J} = \mathbf{U}\boldsymbol{\Sigma}\mathbf{V}^{\mathbf{T}}, \tag{10}$$

where $\mathbf{J}$ is an $M \times N$ Jacobian matrix, $\boldsymbol{\Sigma}$ is an $M \times N$ rectangular diagonal matrix with positive real singular values (σ_i) on the diagonal of the uppermost $N \times N$ part of the matrix, arranged in descending order, $\mathbf{U}$ is an $M \times M$ orthogonal matrix whose orthonormal set of basis vectors corresponding to $\sigma_i \neq 0$ span the range of $\mathbf{J}$, and $\mathbf{V}$ is an $N \times N$ orthogonal matrix whose orthonormal columns correspond to the same numbered $\sigma_i = 0$ are a set of basis vectors spanning the nullspace of $\mathbf{J}$.

Because the matrices $\mathbf{U}$ and $\mathbf{V}$ are both proper orthogonal, then their inverses are equal to their transposes. The matrix $\boldsymbol{\Sigma}$ is diagonal, so its inverse is simply

$$\boldsymbol{\Sigma}^{-1} = \begin{bmatrix} \sigma_1^{-1} & 0 & \cdots & 0 \\ 0 & \sigma_2^{-1} & \cdots & 0 \\ \vdots & & \ddots & \vdots \\ 0 & 0 & & \sigma_n^{-1} \\ 0 & 0 & \cdots & 0 \end{bmatrix}. \tag{11}$$

Then, the Moore-Penrose pseudoinverse of $\mathbf{J}$, can be expressed as [30]

$$\mathbf{J}^{+} = \mathbf{V}\mathbf{\Sigma}^{-1}\mathbf{U}^{\mathbf{T}}. \tag{12}$$

The only time there are computational issues is when one or more of the σ_i are either identically zero, or numerically close to zero, meaning that $\sigma_i^{-1} \rightarrow \infty$. In this case, simply set $\sigma_i^{-1} = 0$. This is not the desperation mathematics it appears to be, and may seem like making a bad situation worse. But, by setting $\sigma_i^{-1} = 0$ below a threshold for σ_i actually eliminates the linear combination of equations that is so corrupted by error that is, at best, useless, because it pushes the solution vector towards infinity in the direction parallel to a nullspace vector. The last column in $\mathbf{V}$ corresponding to the eliminated σ_i gives the elements of $\Delta\boldsymbol{\zeta}$ that are ill-determined even if the system of equations is overdetermined. These elements of $\Delta\boldsymbol{\zeta}$ are insensitive to the data and should be removed [15], [22], [30].

A reasonable threshold stated in [30] is to set $\sigma_i^{-1} = 0$ if

$$\frac{\sigma_i}{\sigma_{max}} < rank(\mathbf{V})\epsilon, \tag{13}$$

where ϵ is the machine precision, typically $\epsilon = 2.2204 \times 10^{-16}$.

C. Numerical Conditioning using SVD

Other than the pseudoinverse, singular value decomposition can also be used as the tool for computing the condition number $\kappa(\mathbf{J})$. The diagonal matrix factor $\mathbf{\Sigma}$ which consists of the singular values of $\mathbf{J}$ has the form

$$\mathbf{\Sigma} = \begin{bmatrix} \sigma_1 & 0 & 0 & \dots & 0 \\ 0 & \sigma_2 & 0 & \dots & 0 \\ \vdots & \vdots & \ddots & \dots & \vdots \\ 0 & 0 & & \dots & \sigma_n \\ 0 & 0 & 0 & \dots & 0 \end{bmatrix}. \tag{14}$$

The condition number of $\mathbf{J}$ is the ratio of the maximum and minimum singular values, and because the singular values are arranged in a descending order, then

$$\kappa(\mathbf{J}) = \frac{\sigma_\mathbf{1}}{\sigma_\mathbf{n}}. \tag{15}$$

Note that the number of $\sigma_i \neq 0$ in $\mathbf{\Sigma}$ is the $rank(\mathbf{J})$.

From Eq. (15), as $\sigma_{n-i} \rightarrow 0$ then $\kappa(\mathbf{J}) \rightarrow \infty$, indicating that the corresponding estimated parameters have been poorly identified. Therefore, replace every $\sigma_i \leq \epsilon$ by 0 increases numerical robustness by removing the influence of near linearly dependent equations.

IV. Experiment and Results

An experiment was set up with a calibration board attached to the end-effector and a camera mounded on a tripod facing the board, similar to that illustrated in Fig. 2. The transformation from the end-effector to the calibration board in the kinematic model using the camera calibration yields the relative measurements that are used to estimate the errors in the controller model of the kinematic geometry of the robot. Table I lists the DH parameters of the 7 DOF WAM Arm using the DH parameters and coordinate reference frames illustrated in Fig. 4. The nominal values of the kinematic parameters are extracted from the WAM arm user manual [31].

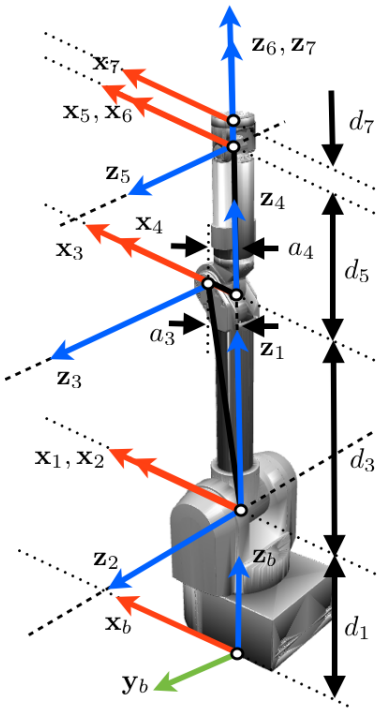

Fig. 4. The DH coordinate frame and parameter assignments of the WAM Arm shown in its zero (home) pose.

Link Number	$\theta_{o,i}$ [deg.]	a_i [mm]	d_i [mm]	α_i [deg.]
Base	0	0	0	0
1	0	0	346	-90
2	0	0	0	90
3	0	45	550	-90
4	0	-45	0	90
5	0	0	300	-90
6	0	0	0	90
7	0	0	60	0
End Link	0	0	0	0

TABLE I. The DH parameters for the 7 DOF WAM Arm.

Before calibrating the robot, a set of robot poses are needed. Since the WAM Arm consists of 7 serially connected revolute joints, then each pose is defined by 7 joint angles. The next section describes how the joint angles are generated to define a useful set of robot poses.

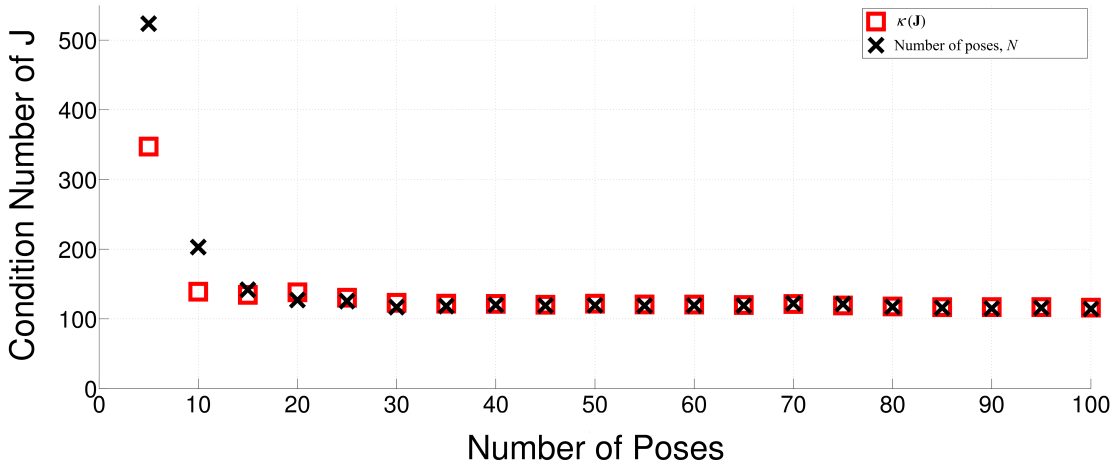

Fig. 5. The number of poses verses the condition number of the Jacobian.

A. *Generating Poses for Kinematic Calibration*

The number of measurement poses required for the kinematic calibration depends on the number of parameters being identified and the existing measurement error in the system. The analysis for determining the number of required measurement poses is rigourously described in [32] and briefly summarized in what follows. The identied kinematic parameters are generally affected by the presence of measurement noise, but the precision of the identied errors can generally be improved by increasing the number of poses that are measured. Fig. 5 is intended to illustrate the effect of increasing the number of measurements on the goodness of identication implied by the condition number of the corresponding identification Jacobian, $\mathbf{J}$. Note that the kinematic geometry driving this examination was that of a Thermo CRS A465, but the trend revealed applies to all serial arms. In a simulation, 100 poses were generated by randomly choosing the joint angles within the manipulators joint limits. These joint angles and $\boldsymbol{\zeta}_A$ are specified at the start of the simulation program, and they do not change throughout the analysis. The number of poses, N, in Fig. 5 are extracted from the 100 randomly generated poses, where N poses refers to the first N poses out of all 100. The simulation analysis strictly involves varying the number of poses only.

Using standard DH parameters to describe the kinematic geometry of the six-axis Thermo CRS A465 means that there are 28 parameter errors to be identified. Each pose measurement yields six equations. This means that at least five poses, yielding 30 equations are required, giving an over-determined set of equations to solve for the 28 parameter errors. Examining Fig. 5, the first point represents those five measurement poses and the corresponding Jacobian condition number. The figure illustrates that there is a diminishing return in this relationship, as the $\kappa(\mathbf{J})$ appears to converge to a relatively stable number after 40 pose measurements.

The trajectory of the poses in the workspace can also contribute to the success in identifying kinematic parameters, because some of the parameters are unobservable in certain configurations. Again, analyses made in [32] was used for determining a suitable set of configurations for successful kinematic calibration, but the results are too lengthy to summarize here. Regardless, the results showed that the best sequence of poses is one that spans the width of the robot's 3D reachable workspace.

Respecting the considerations above, a simulation was made to generate suitable joint angles for an experiment. Fig. 6 illustrates the first 15 out of 100 simulated configurations of the WAM Arm. In this simulation, the manipulator base was placed at the Cartesian coordinates $(0, 0, 0)$, and the coordinates of origin of the camera coordinate reference frame was placed at $(-1.5, 0.5, 0.3)$ relative to the base, where units are meters.

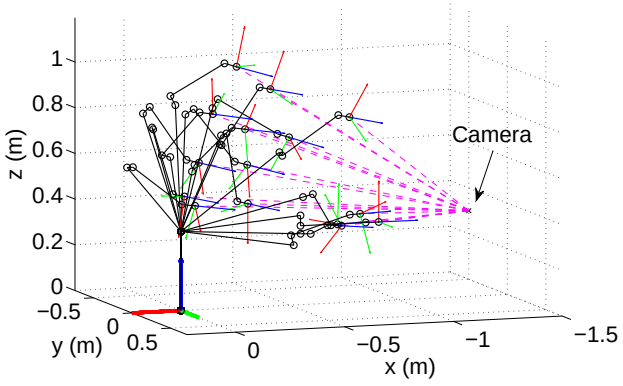

Fig. 6. The kinematic model of the WAM in simulation.

	Joint Errors [deg]		Link Errors [mm]	
	$\Delta\boldsymbol{\theta}_{id}$	$\Delta\boldsymbol{\alpha}_{id}$	$\Delta\boldsymbol{a}_{id}$	$\Delta\boldsymbol{d}_{id}$
b	0.3125	−2.1665	N.A.	N.A.
1	−0.7545	−0.6120	3.5969	N.A.
2	0.1178	0.0489	−0.4241	0.2090
3	2.7705	−0.4397	−3.7679	−17.6295
4	0.5644	−0.2677	−1.3260	−10.1315
5	−1.4946	0.8305	5.4388	−24.2630
6	−3.5829	−0.3029	−4.2547	−7.6065
7	61.8989	4.2142	2.7863	45.8806
n	N.A.	0.5255	−82.9751	N.A.

TABLE II. Experimental results for the calibration using relative measurements.

B. Kinematic Calibration Results For the WAM Arm

Using the generated set of 40 joint angles and the corresponding pose relative measurements obtained using the adapted camera calibration algorithm from [32], the experimental data was acquired and processed yielding the results listed in Table II. There are 36 kinematic parameter errors to identify, meaning that the rank of $\mathbf{J}$ should be 36. However, $rank(\mathbf{J})$ turned out to be 31, implying that the five smallest singular values in $\boldsymbol{\Sigma}$ are either identically zero, or perilously close to the numerical resolution of the computer. The parameters in $\mathbf{V}$ with corresponding indices are the unobserved parameters. The equations containing these five parameters are therefore linearly dependent and should be eliminated from the system of equations. Hence, after removing the five columns of $\mathbf{J}$ associated with the parameters Δa_b, Δd_b, Δd_1, $\Delta\theta_n$, and Δd_n, the recalculated rank remained $rank(\mathbf{J}) = 31$ and the recalculated condition number was $\kappa(\mathbf{J}) = 208.88$, which means that the remaining 31 parameter erors are reasonably well identified in the context of the kinematic model. Note that some of the the unexpectedly large errors in Table II are partly an artifact of the WAM Arm joint angles having not been mastered[1]. The unobserved parameter errors in Table II are listed as N.A., for *not available*. As expected, the positional components of the manipulator base (Δa_b, Δd_b, and Δd_1) were not identified because these parameters are unobservable using relative measurements [32].

Fig. 7 illustrates the first 15 end-effector positions before robot calibration, and Fig. 8 illustrates the first 15 end-effector positions after correcting the kinematic model for the errors listed in Table II. The overall improvement in robot positioning and orienting accuracy was estimated using the root-mean square error in each pose, comparing the prescribed and attained positions and orientations. By using the RMC calibration, those accuracies improved from

[1] A mastering procedure identifies the relationship between the position sensor attached to each motor and each axis angle defined for the robot [1].

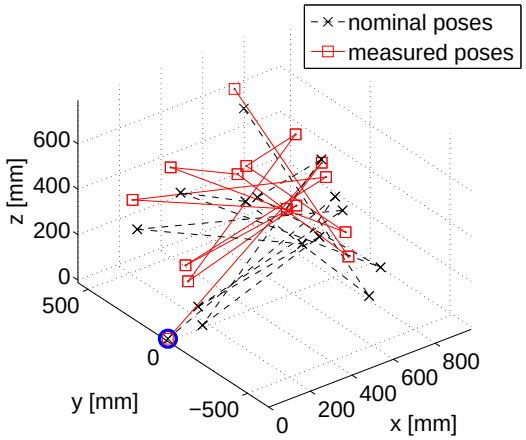

Fig. 7. Measured and nominal relative positions before calibration.

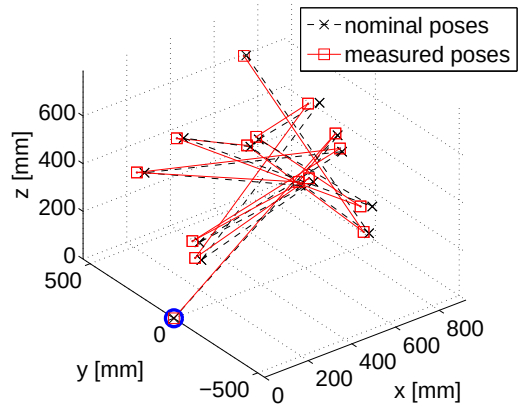

Fig. 8. Measured and nominal relative positions after calibrtion.

± 3.150 mm and $\pm 0.329°$ to ± 1.055 mm and $\pm 0.200°$, respectively, averaged over the 40 prescribed poses. Recall that the repeatability for the WAM Arm is ± 0.2 mm, implying the precision of these results need improvement. Regardless, the accuracy has been enhanced in this case.

V. Conclusions

In this paper a kinematic calibration method for serial manipulators using the relative measurement concept was developed and implemented. Relative measurements were used in the kinematic calibration algorithm instead of absolute measurements. The results presented herein are the first empirical validation in the published literature, to the best of the authors knowledge, that relative measurements are capable of enhancing the positioning and orienting accuracy of a serial robot manipulator.

Arguably, relative measurements are easier and less expensive to make compared to absolute measurements. Furthermore, the RMC presented here is straightforward to im-

plement on a production line or manufacturing floor and can easily be applied to any serially connected robotic manipulator. The system is also task-specific, meaning a robot can be calibrated with the appropriate tool and over the task-space being used, as opposed to the entire workspace, thereby correcting geometric errors and improving position and orientation accuracy without the need to absolutely measure arbitrary poses covering the reachable workspace of the robot.

An open question is "how well does the RMC preform compared to the AMC over a prescribed set of poses?". This is the subject of our future work. Comparable calibration methods that employ absolute measurement systems will be investigated. Experimental test plans will then be developed to attempt to reproduce the published results using the relative measurement procedure adapted to obtain comparable results. If the RMC yields comparable calibration results as the AMC, this will be an important result because of its flexibility, ease of implementation, and relative expense.

References

[1] Z.S. Roth, B.W. Mooring, and B. Ravani. An overview of robot calibration. *IEEE J. Robotics and Automation*, pages 1690-1695, Scottsdale, AZ, 1989.

[2] R.P. Judd, and A.B. Knasinski. A technique to calibrate industrial robots with experimental verification. In *Proceedings of the 1987 IEEE International Conference on Robotics and Automation*, pp. 183-189, April 1987.

[3] I.-M. Chen, G. Yang, C.T. Tan, and S.H. Yeo. Local POE model for Robot Kinematic Calibration. *Mechanism and Machine Theory*, pp. 1215-1239, 2001.

[4] Y. Lou, T. Chen, Y. Wu, and G. Liu. Computer Vision Based Calibration of the Purely Translational Orthopod Manipulator. *Proceedings of the 2009 IEEE International Conference on Information and Automation*, June 2009.

[5] Y. Meng, and H. Zhuang. Self-Calibration of Camera-Equipped Robot Manipulators. *The International Journal of Robotics Research*, November 2001.

[6] I.-W. Park, B.-J. Lee, S.-H., Y.-D. Hong, and J.-H. Kim. Laser-Based Kinematic Calibration of Robot Manipulator Using Differential Kinematics. *IEEE/ASME Transactions on Mechatronics*, 2012.

[7] H. Zhuang, W.-C. Wu, and Z.S. Roth. Camera-Assisted Calibration of SCARA Arms. *Proceedings IEEE/RSJ International Conference on Intelligent Robots and Systems, Human Robot Interaction and Cooperative Robotics*, 1995.

[8] A. Nubiola and I.A. Bonev. Absolute Calibration of an ABB IRB 1600 Robot Using a Laser Tracker. *Robotics and Computer-Integrated Manufacturing*, Vol. 29, No. 1, pp. 236-245, February 2013.

[9] L.J. Everett, M.R. Driels, and B.M. Mooring. Kinematic modelling for robot calibration. *Proceedings of the 1987 IEEE International Conference on Robotics and Automation*, pp. 183-189, April 1987.

[10] C.H. Wu. A Kinematic CAD Tool for the Design and Control of a Robot Manipulator. *The International Journal of Robotics Research*, 3(1), pp. 58-67, 1984.

[11] H.S. Lee, S.L. Chang. Development of a CAD/CAE/CAM System for a Robot Manipulator. *The Journal of Materials Processing Technology*, pp. 100-104, 2003.

[12] H. Hage, P. Bidaud, and N. Jardin, Practical Consideration on the Identification of the Kinematic Parameters of the Staübli TX90 Robot. 13^{th} *World Congress in Mechanism and Machine Science*, Guanajuato, Mexico, 2011.

[13] D. Wang, Y. Bai, and J. Zhao. Robot Manipulator Calibration using Neural Network and a Camera-Based Measurement System. *Transactions of the Institute of Measurement and Control*, 2010.

[14] M.J.D. Hayes and P.L. O'Leary. Kinematic Calibration Procedure for Serial Robots with Revolute Axes. *Technical Report*, Institute for Automation, University of Leoben, April 12, 2001.

[15] K. English, M.J.D. Hayes, M. Leitner, C. Sallinger. Kinematic Calibration of Six-Axis Robots. *Proceedings of the CSME Forum 2002*, Queen's University, Kingston, ON, Canada, on CD, May, 2002.

[16] N.W. Simpson. Kinematic calibration of 6-axis serial robots using the relative measurement concept. *M.Eng. Thesis, Carleton University*, 2004.

[17] I.-C. Ha. Kinematic parameter calibration method for industrial robot manipulator using the relative position. *Journal of mechanical science and technology*, Springer, 2008.

[18] J.S. Shamma, and D.E. Whitney. A Method for Inverse Robot Calibration. Transactions of the ASME *Journal of Dynamic Systems, Measurements, and Control*, vol. 109, pp. 36-43, 1987.

[19] A. Doria, F. Angrilli, and S. de Marchi. Inverse Kinematics Robot Calibration by Spline Functions. *Applied Mathematical Modelling*, Vol. 17, No. 9, pp. 492-498, September 1993.

[20] X. Zhong, J. Lewis, and F.L. N-Nagy. Inverse Robot Calibration using Artificial Neural Networks. *Engineering Applications and Artificial Intelligence*. Vol. 9, No. 1, pp. 83-93, 1996.

[21] J.U. Dolinsky. The development of a genetic programming Method for kinematic robot calibration. *John Moores University, Liverpool, U.K.*, 2001.

[22] B.W. Mooring, Z.S. Roth, and M.R. Driels. Fundamentals of Manipulator Calibration. *John Wiley Sons, Inc.*, 1991.

[23] H.W. Stone. Kinematic Modeling, Identification, and Control of Robotic Manipulators. *Kluwer Academic Publishers*, Boston, 1987.

[24] M.E. Sklar. Metrology and Calibration Techniques for the Performance Enhancement of Industrial Robots. *PhD. thesis, University of Texas at Austin*, Austin, Texas, 1988.

[25] M.E. Sklar. Geometric calibration of industrial manipulators by circle point analysis. *Proceedings of Second Conference on Recent Advances in Robotics*, pp. 178-202, Florida Atlantic University, May, 1989.

[26] M.S. Kim, H.S. Yoo, S.W. Cho, H.S. Change, and G. Spur. A New Calibration Method. *Annals of the CIRP*, Vol. 39. January, 1990.

[27] Denavit, J., Hartenberg, R.S. A Kinematic Notation for Lower-Pair Mechanisms Based on Matrices. *J. of Applied Mechanics*, pp. 215-221, 1955.

[28] G. Bradski, and A. Kaehler. *Learning OpenCV*. Published by O'Reily Media Inc., 2005.

[29] C.C.D. Lu, and M.J.D. Hayes. Kinematic Calibration of 6R Serial Manipulators Using Relative Measurements. *Proceedings of the 8th CCToMM Symposium on Mechanisms, Machines, and Mechatronics*, École de technologie supérieure, Montréal, QC, Canada, May 30-31, 2013.

[30] W.H. Press, S.A. Teukolsky, W.T. Vetterling, and B.P. Flannery. *Numerical Recipes in C: The Art of Scientific Computing.* Cambridge University Press, 2^{nd} edition, 1992.

[31] Barrett Technology Inc.. $A465$ *Robot System Guide*. July 2002.

[32] C.C.D. Lu. *Kinematic Calibration of Serial Manipulators using Relative Measurements*. M.A.Sc. Thesis, Carleton University, 2014.